

Preferential cell response to anisotropic electro-spun fibrous scaffolds under tension-free conditions

A. English · A. Azeem · D. A. Gaspar ·
K. Keane · P. Kumar · M. Keeney ·
N. Rooney · A. Pandit · D. I. Zeugolis

Received: 16 August 2011 / Accepted: 24 October 2011 / Published online: 22 November 2011
© Springer Science+Business Media, LLC 2011

Abstract Anisotropic alignment of collagen fibres in musculoskeletal tissues is responsible for the resistance to mechanical loading, whilst in cornea is responsible for transparency. Herein, we evaluated the response of tenocytes, osteoblasts and corneal fibroblasts to the topographies created through electro-spinning and solvent casting. We also evaluated the influence of topography on mechanical properties. At day 14, human osteoblasts seeded on aligned orientated electro-spun mats exhibited the lowest metabolic activity ($P < 0.001$). At day 5 and at day 7, no significant difference was observed in metabolic activity of human corneal fibroblasts and bovine tenocytes respectively seeded on different scaffold conformations ($P > 0.05$). Osteoblasts and corneal fibroblasts aligned parallel to the direction of the aligned orientated electro-spun mats, whilst tenocytes aligned perpendicular to the aligned orientated electro-spun mats. Mechanical evaluation demonstrated that aligned orientated electro-spun fibres exhibited significant higher stress at break values than their random aligned counterparts ($P < 0.006$) and random orientated electro-spun fibres

exhibited significant higher strain at break values than the aligned orientated scaffolds ($P < 0.006$). While maintaining fibre structure, we also developed a co-deposition method of spraying and electro-spinning, which enables the incorporation of microspheres within the three-dimensional structure of the scaffold.

1 Introduction

Nature shows strong preference for bottom up design to build hierarchically ordered tissues. In the case of tendon, for example, cells synthesise procollagens with intact propeptide extensions. Following or during secretion, specific propeptide cleavage by specific proteinases takes place, which triggers the spontaneous quarter-staggered assembly of collagen molecules to elongated collagen fibrils. Following fibril formation, the lysyl-oxidase cross-linking pathway takes place in a head-to-tail fashion to form fibres that will subsequently form fibre bundles and finally a tendon unit [1]. This naturally engineered collagen conveys load bearing functionality to tissues such as tendon and bone [2], whilst in the case of cornea the high degree of structural organisation and alignment facilitates transparency [3]. To successfully build biomimetic tissue equivalents that will repair or replace injured or degenerated tissues, it is essential to recapitulate this fundamental structural hierarchy.

A number of nano- and micro-fabrication technologies are available to-date to build biomimetic three dimensional tissue analogues [4, 5]. Among them, electro-spinning has emerged as a scaffold fabrication technique that enables production of fibres that closely imitate the length and diameter of native collagen fibres. The use of extracellular matrix biopolymers has been restricted as harsh solvents are often required to perform electro-spinning successfully

A. English · A. Azeem · D. A. Gaspar · K. Keane · P. Kumar ·
M. Keeney · A. Pandit · D. I. Zeugolis (✉)
Network of Excellence for Functional Biomaterials (NFB),
National University of Ireland Galway (NUI Galway),
Galway, Ireland
e-mail: dimitrios.zeugolis@nuigalway.ie

A. English · A. Azeem · K. Keane · P. Kumar · D. I. Zeugolis
Department of Mechanical & Biomedical Engineering,
NUI Galway, Galway, Ireland

M. Keeney
Department of Orthopaedic Surgery, Stanford University,
Stanford, CA 94305, USA

N. Rooney
Proxy Biomedical, Galway, Ireland

[6, 7]. To-date, numerous polymers have been utilised to produce scaffolds of various topographies for neural [8, 9], tendon [10, 11], bone [12, 13], cartilage [14, 15] and cardiovascular [16, 17] applications.

Biomaterials design has evolved from basic constructs that match structural and mechanical properties, to biofunctional materials that aim to incorporate instructive signals into scaffolds and to modulate cellular functions such as proliferation, differentiation and morphogenesis [18, 19]. Indeed, the emerging field of tissue engineering requires accurate delivery of bioactive and/or therapeutic molecules to a specific location. To this end, the use of polymeric delivery vehicles in the form of micro- or nano-spheres/particles to encapsulate the active molecules and maintain a sustained localised delivery to the target site is attractive [20–22].

Despite the significant advancements that have been achieved, the influence of scaffold topography on the biomechanical properties and cell response has not been fully investigated. Moreover, electro-spun mats functionalisation is primarily carried out by blending the polymer and the molecule of interest together. However, such method offers little control over the release of the loaded molecules; may jeopardise the mechanical properties of the scaffold; and is also characterised by limited miscibility between the solution containing the molecule of interest and the solvent used to dissolve the polymer [23, 24]. Thus, herein we ventured to evaluate the influence of various scaffolds topographies on the mechanical properties of the scaffolds and evaluate bovine tenocytes, human osteoblasts and human corneal fibroblasts response as a function of topography. In addition, we developed a technique that enables simultaneous electro-spinning and micro-sphere spraying and allows the incorporation of microspheres within the three-dimensional structure of the scaffold.

2 Materials and methods

2.1 Materials

Poly(glycolide-co-lactide) 85/15 (PLGA) was purchased from Purac Biomaterials (Gorinchem, Netherlands). AlamarBlue[®] cell metabolic activity kit was purchased from BioSource International, Invitrogen (Dun Laoghaire, Ireland). Tissue culture consumables were purchased from Sarstedt (Wexford, Ireland) and Nunc (Roskilde, Denmark). All other materials were purchased from Sigma Aldrich (Wicklow, Ireland), unless otherwise stated.

2.2 Scaffold fabrication

The electro-spinning set-up consisted of a high voltage power supply (Gamma High Voltage, USA), a syringe

pump (NE-1000, New Era Pump Systems Inc., USA) and a custom-made circular drum (10 cm in diameter) covered with aluminium foil, which acted as a collector. Eight percentage w/v PLGA solution in chloroform was prepared after overnight orbital stirring using a Stuart[®] SB3 rotator (Bidby Scientific Limited, UK). Polymer solutions were loaded into a 10 ml syringe (BD and Company, Ireland) fitted with an 18G stainless steel needle (BD and Company, Ireland). Upon application of high voltage between the needle and the collector (18 cm distance), the solvent was evaporated and the fibres were collected on the drum. At 1,300 rpm aligned fibrous mats were obtained, whilst at 200 rpm non-aligned fibrous mats were obtained. Solvent casted PLGA (8% w/v in chloroform) was used as control scaffold with no topographical features (i.e. smooth surface). The polymer solution was gently poured into aluminium foil trays, avoiding bubble formation. The trays were covered with another layer of aluminium foil to control the evaporation rate of the solvent.

2.3 Functionalisation using microspheres

PLGA microspheres were fabricated using a single-emulsion solvent evaporation technique as has been described before [25]. Briefly, using a T25 digital UltraTurrax[®] homogenizer, 40 ml of 4% v/w PLGA/chloroform solution was gradually added to a stirring 300 ml solution of 0.5% polyvinyl alcohol. The resulting emulsion was stirred for 6 h at 600 rpm and hardened spheres were subsequently collected. The sphere solution was then centrifuged at 1,200 rpm for 5 min. The spheres were resuspended in isopropyl alcohol and placed into spray bottles. To embed the spheres into the electro-spun mats, the rotating drum was sprayed with the sphere solution during the electro-spinning process.

2.4 Scanning electron microscopy analysis

The morphology of the produced scaffolds was evaluated using a low voltage, high resolution Scanning Electron Microscope (SEM; S-4700 Hitachi Scientific Instruments, Berkshire, UK) after gold sputtering (Emitech K-550 × Sputter Coater, Emitech Ltd., Ashford, Kent, UK).

2.5 Biophysical evaluation

Stress–strain curves of dry and wet electro-spun PLGA mats were determined in uniaxial tension using a Zwick Z2.5 Universal Mechanical Tester (Bratislava, Slovakia) at a crosshead speed of 10 mm/min using a 100 N load cell, as has been described previously [26–29]. To avoid damaging the electro-spun mats during handling, the mats were mounted on a paper frame as has been described before [30, 31]. The gauge length was determined by the vertical

dimension of the window in the frame (3 cm in length). Frames containing specimen mats were then placed between the upper and lower grips of the Zwick. The sides of the frame were then cut leaving the specimen intact. The width of the samples was fixed at 1 cm. The thickness of the samples was determined using a digital micro-meter (Tresna, Essen, Germany) with an accuracy of 1 μm ; three readings were taken for each sample. Results obtained with electro-spun mats that broke at contact points with the grips were rejected. The following definitions were used to calculate the mechanical data: stress at break was defined as the load at complete failure divided by the original cross-sectional area (engineering-stress); strain at break was defined as the increase in fibre length required to cause failure divided by the original length and Young's modulus of samples was calculated from slope of the stress strain curve in the linear region and the initial sample geometry. Prior to wet testing, dry electro-spun mats were equilibrated in PBS (0.01 M; pH 7.4) at room temperature overnight.

2.6 Bovine tenocyte isolation

Bovine hind limbs were sourced from a local abattoir. Using aseptic techniques the tendons were isolated from the surrounding fascia and tenocytes were isolated as has been described previously [32]. Briefly, the limbs were washed with PBS and prepared for incision. The skin was then washed further with 70% ethanol. With disposable scalpel each layer of skin and soft tissue was released and retracted. The tendon was then transected a quarter away from the insertion and musculotendinous junction. The tendons were subsequently placed into sterile Hanks Balanced Salt Solution (HBSS) and stored in ice. Following that, the tendons were placed into a petri dish with a small volume of ice cold HBSS and diced to approximately 2 mm by 2 mm pieces. The tendon pieces were then digested with filtered 0.15% collagenase solution into 50 ml centrifuge tubes. The solution was stored under agitation in an incubator maintained at 37°C and 5% CO₂ overnight. The following day, the solution was passed through a nylon mesh cell strainer to remove any matrix debris or undigested material and filtrate-centrifuged at 1,200 rpm for 5 min. The cell pellet was resuspended in culture media and seeded into 175 cm² tissue culture flasks. Bovine tenocytes were then cultured as described below.

2.7 Culture of bovine tenocytes

Freshly isolated bovine tenocytes were cultured in Dulbecco's modified Eagle's medium (DMEM) supplemented with 10% Foetal Bovine Serum (FBS) and 1% penicillin/streptomycin in 75 cm² flasks. The bovine tenocyte culture was maintained at 37°C in a humidified 5% CO₂ incubator until they were approximately 80% confluent with media

being changed every 2–3 days. At passage 3, 1.5×10^4 cells/cm² cells were seeded on the various scaffolds conformations (PLGA aligned and randomly orientated electro-spun mats and solvent cast films) for 2, 4 and 7 days.

2.8 Culture of human osteoblasts

Primary human osteoblasts (Cat. No: CC-2538, Lonza, USA) were cultured in low glucose Dulbecco's modified Eagle's medium (DMEM) supplemented with 10% Foetal Bovine Serum (FBS) and 1% penicillin/streptomycin. The osteoblast culture was maintained at 37°C in a humidified 5% CO₂ incubator until they were approximately 80% confluent with media being changed every 2–3 days. Human osteoblasts (passages 4–5) were seeded for 2, 5 and 14 days on various substrates (e.g. PLGA aligned and randomly orientated electro-spun mats and solvent cast films) in 24-well plates at 1.5×10^4 cells/cm² density.

2.9 Culture of human corneal fibroblast

Primary human corneal fibroblasts (Cat. No: P10872, Innoprot Inc., Derio-Bizkaia, Spain) were cultured as per supplier protocol. Briefly 5,000 cells/cm² were seeded in poly-L-Lysine coated T-75 flasks in fibroblast culture medium kit (Cat No P60108, Innoprot Inc, Derio-Bizkaia, Spain) composed of 2% foetal bovine serum, fibroblast growth supplement, 1% penicillin/streptomycin and fibroblast medium buffered with HEPES and bicarbonate. The cells were maintained in 5% CO₂ in humidified incubator at 37°C. The medium was replaced with fresh one after 24 h and after that every 2–3 days. When the cells reached confluency, were subcultured until sufficient numbers were obtained. Subsequently, human corneal fibroblasts (passage 4) were seeded for 1, 3 and 5 days on the various substrates (e.g. PLGA aligned and randomly orientated electro-spun mats and solvent cast films) in 24-well plates at 20,000 cells/cm² in keratocyte medium composed of DMEM/F12, 5 ng/ml of basic fibroblast growth factor, 10% new born calf serum and 1% penicillin/streptomycin as has been described before [33, 34].

2.10 Cell metabolic activity

Cell metabolic activity was determined using alamarBlue[®] cell metabolic assay at predetermined time depending on cell type (mentioned above for the different cell types). Briefly, alamarBlue[®] dye was diluted with Hank's Balance Salt Solution to make a 10% (v/v) alamarBlue[®] solution. Media was removed from each well and 0.5 ml Alamar Blue[®] solution was added to each well. Depending on cell type after

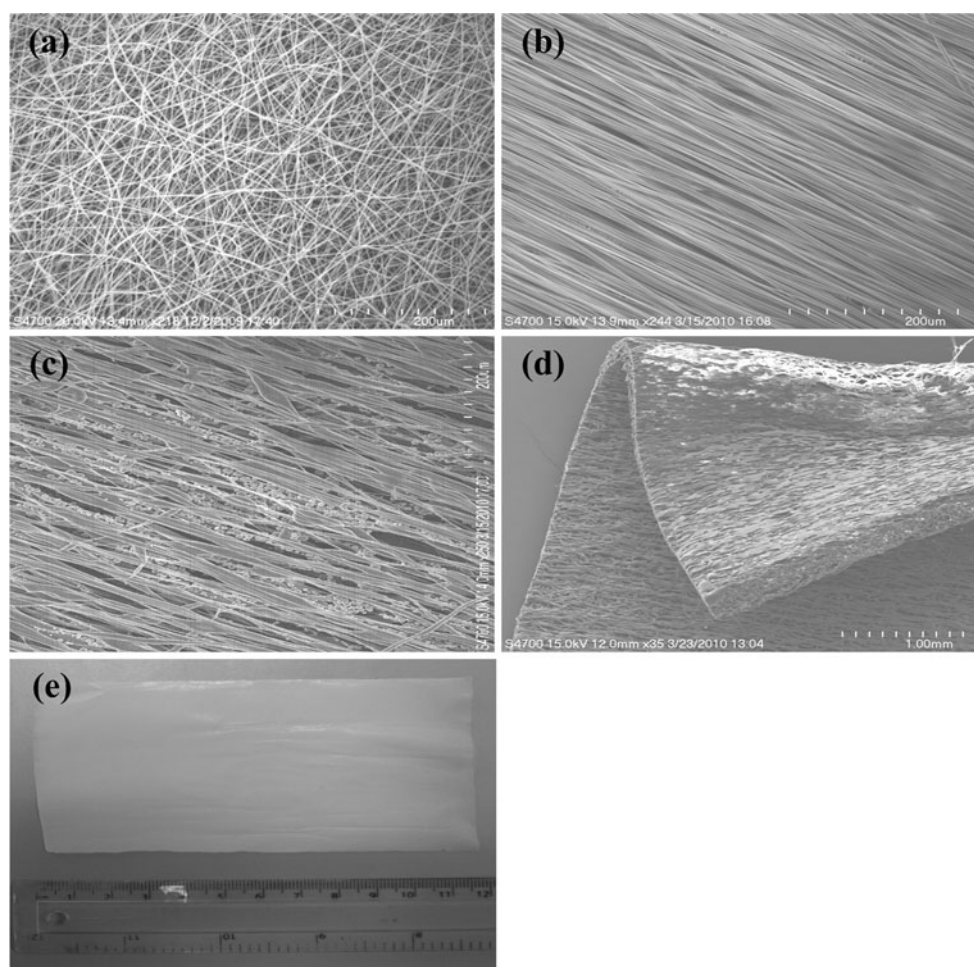


Fig. 1 Scanning electron micrographs of random and aligned oriented electro-spun scaffolds (**a**, **b** respectively). Scanning electron micrographs of mono-dispersed microspheres embedded within

aligned oriented electro-spun scaffolds (**c**). Scanning electron (**d**) and optical (**e**) micrographs of three-dimensional aligned oriented nano-structured composites

an incubation time of between 1 and 4 h at 37°C, the absorbance was measured at wavelengths of 550 and 595 nm using a microplate reader (Varioskan Flash, Thermo Scientific). The level of metabolic activity was calculated using the simplified method of calculating per cent reduction, according to the supplier's protocol. The metabolic activity of cells at solvent cast film at day 2 was considered as 100%.

2.11 Cell fluorescent labelling

Cell attachment, spreading and alignment was assessed by using immunofluorescent images. Briefly, the cells (tenocytes, osteoblasts and corneal fibroblasts) were fixed with 4% paraformaldehyde for 15 min, permeabilised with 0.2% TritonX, and the nucleus was stained with 4',6-Diamidino-2-phenylindole (DAPI, Molecular Probes) for 5 min. The actin cytoskeleton of the cells was then stained with rhodamine conjugated phalloidin (Molecular Probes) for 1 h.

Images were captured at 10 × magnification using an inverted BX51 Olympus fluorescence microscope.

2.12 Statistical analysis

Numerical data is expressed as mean ± SD. Analysis was performed using statistical software (MINITAB™ version 16, Minitab, Inc., State College PA, USA). Two sample t-test for pairwise comparisons was employed after confirming the following assumptions: (a) the distribution from which each of the samples was derived was normal (Anderson–Darling normality test); and (b) the variances of the population of the samples were equal to one another (Bartlett's and Levene's tests for homogeneity of variance). Non-parametric statistics were utilised when either or both of the above assumptions were violated and consequently Mann–Whitney test for two samples was carried out. Statistical significance was accepted at $P < 0.05$.

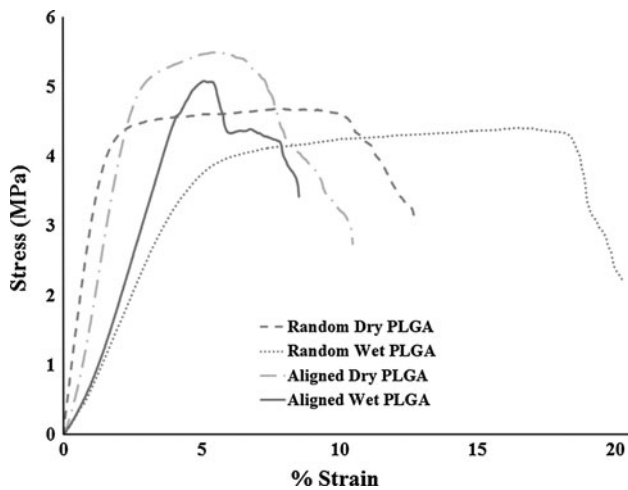


Fig. 2 Stress-strain curves of dry and wet aligned and random orientated electro-spun fibrous mats. Aligned electro-spun mats in dry and wet state exhibited a region of rising stress, followed by a region of decreasing stress, whilst random electro-spun mats in dry and wet state revealed a region of rising stress, followed by a region of constant gradient and then a region of decreasing stress, which persisted up to the point of fracture

3 Results

3.1 Scaffold morphology

SEM analysis revealed that all electro-spun mats were composed of uniform (no bids) random and aligned orientated fibres (Fig. 1a, b respectively) Mono-dispersed microspheres were also produced and successfully incorporated into the produced aligned orientated electro-spun mats (Fig. 1c). Continuous electro-spinning gave rise to a three-dimensional scaffold (Fig. 1d, e).

3.2 Biophysical analysis

Uniaxial tensile tests of aligned orientated electro-spun mats in both wet and dry state exhibited stress–strain curves consisting of a region of steeply rising stress, followed by a region of decreasing stress up to the point of fracture (Fig. 2). Uniaxial tensile tests of randomly orientated electro-spun mats in both wet and dry state exhibited stress–strain curves consisted of a region of steeply rising stress, followed by a region of constant gradient and then a

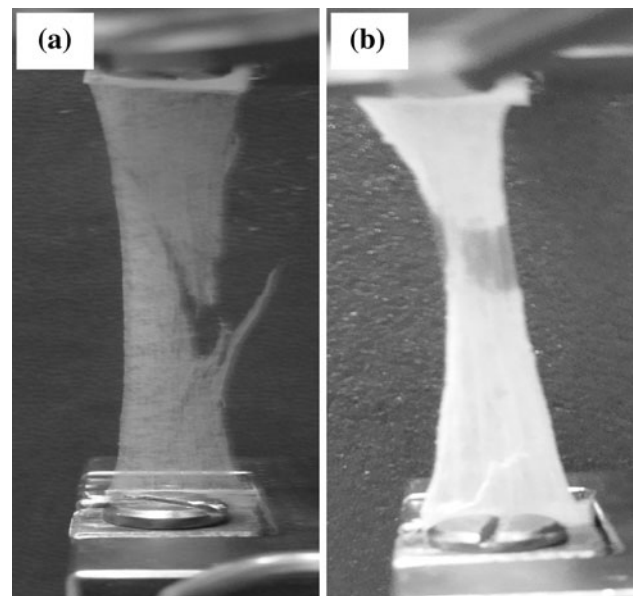


Fig. 3 Fibre orientation resulted in different deformation mechanisms. Aligned orientated electro-spun mats **a** exhibited a split fracture mode, whilst random orientated electro-spun mats **b** displayed a delayed split fracture mode

region of decreasing stress, which persisted up to the point of fracture (Fig. 2). These distinct deformation mechanisms can be visually observed in Fig. 3, where aligned electro-spun mats exhibited a split fracture mode, whilst their random orientated counterparts demonstrated a delayed split fracture mode.

Table 1 summarises the mechanical properties of the electro-spun mats produced in this study. In the dry state, random and aligned orientated electro-spun mats demonstrated no significant difference in thickness, stress at break and modulus values ($P > 0.05$), whilst significant difference in strain at break values was observed ($P < 0.001$). In the wet state, random and aligned orientated electro-spun mats demonstrated no significant difference in thickness ($P > 0.05$), whilst significant difference was observed between stress and strain at break and modulus values ($P < 0.006$).

3.3 Biological evaluation

Cell–matrix interactions between different cell-types and different substrates were studied in vitro by seeding bovine

Table 1 Mechanical properties of dry and wet random and aligned orientated PLGA electro-spun mats

Scaffold conformation and state	Thickness (μm) \pm SD	Stress at break (MPa) \pm SD	% Strain \pm SD	Modulus (MPa) \pm SD
Random dry PLGA mats ($n = 5$)	38.40 \pm 2.70	3.14 \pm 1.15	17.09 \pm 2.20	1.61 \pm 0.69
Aligned dry PLGA mats ($n = 5$)	37.80 \pm 5.03	3.20 \pm 0.42	10.38 \pm 1.34	1.69 \pm 0.78
Random wet PLGA mats ($n = 4$)	43.00 \pm 8.25	2.66 \pm 0.44	23.66 \pm 7.67	0.96 \pm 0.46
Aligned wet PLGA mats ($n = 6$)	33.72 \pm 5.47	3.98 \pm 0.61	9.32 \pm 1.07	1.71 \pm 0.56

Sample number n in parentheses, SD standard deviation

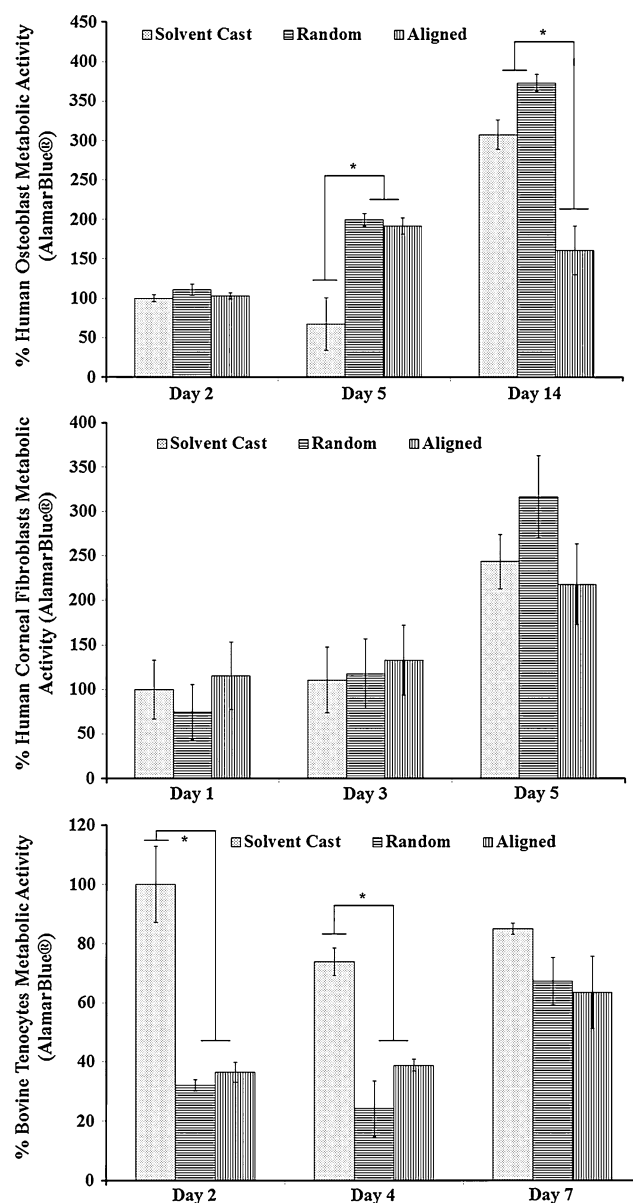


Fig. 4 AlamarBlue® metabolic activity assay results for all cell types and time points. At day 14, human osteoblasts seeded on aligned orientated electro-spun mats exhibited the lowest metabolic activity ($P < 0.001$). At day 1, 3 and 5, no significant difference was observed in metabolic activity of human corneal fibroblasts seeded on different scaffold conformations ($P > 0.05$). No significant difference in metabolic activity of bovine tenocytes was observed among the different scaffold conformations by day 7 ($P > 0.05$). The metabolic activity was also increased for all cells seeded on the various substrates as a function of time. *: Indicates significant difference

tenocytes, human osteoblasts and human corneal fibroblasts on the produced scaffolds for various time periods. Figure 4 shows results of the AlamarBlue® metabolic activity assay. At day 2, no significant difference was observed in metabolic activity of human osteoblasts seeded on different scaffold conformations ($P > 0.05$). At day 5, human osteoblasts seeded on both electro-spun mats

conformations exhibited significant higher metabolic activity that cells seeded on solvent casted films ($P < 0.001$). On day 14, human osteoblasts seeded on aligned orientated electro-spun mats exhibited the lowest metabolic activity ($P < 0.001$). At day 1, 3 and 5, no significant difference was observed in metabolic activity of human corneal fibroblasts seeded on different scaffold conformations ($P > 0.05$). At day 2 and 4, bovine tenocytes seeded on solvent casted films exhibited significant higher metabolic activity than cells seeded on either of the electro-spun mats ($P < 0.001$). However, no significant difference in metabolic activity was observed among the different scaffold conformations by day 7 ($P > 0.05$).

Bovine tenocytes exhibited a random cytoskeleton and nuclei conformation, when they were seeded on solvent casted films and random orientated electro-spun mats for all the time points evaluated. However, they appeared to orientate perpendicularly to the substrate topography, when they were seeded onto aligned orientated electro-spun mats (Fig. 5).

Human osteoblasts (Fig. 6) and corneal fibroblasts (Fig. 7) exhibited a random cytoskeleton and nuclei conformation, when they were seeded on solvent casted films and random orientated electro-spun mats. However, when aligned orientated electro-spun mats were used, cytoskeleton and nuclei orientated parallel to the substrate topography.

4 Discussion

Nano-scale technologies are emerging as powerful tools for tissue engineering and biological studies due to their ability to operate on the same small scale as all functions involved in the growth, development and ageing of the human body [35]. Biomaterials design is now required to include topographical cues, since topography offer control over cellular functions such as growth, directional cell motility, tissue development, angiogenesis and immune response [36–47]. The rationale of this approach is based on the fact that basement membranes are covered with grooves, ridges, whorls, pits, pores and intertwined fibrillar meshwork of the extracellular matrix [18, 48, 49]. Biomaterials are also required to accurately deliver bioactive and/or therapeutic molecules to a specific location in order to protect the typically labile molecules and to positively interact with host and enhance tissue repair and regeneration [50–52]. Herein, we evaluate the effect of electro-spinning- and solvent casting- induced topographies on the metabolic activity and alignment of human osteoblasts and corneal fibroblasts and bovine tenocytes and we describe a method consisting of electro-spinning and spraying to introduce a further element of functionality to the three-dimensional scaffold.

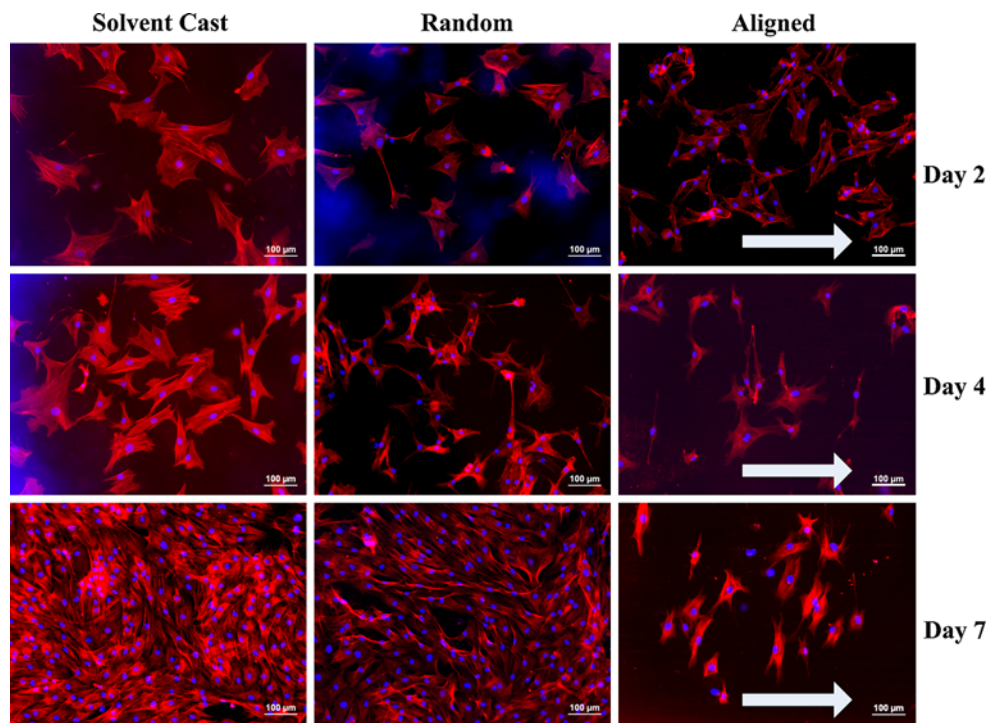


Fig. 5 Bovine tenocytes were seeded on solvent casted and random orientated electro-spun mats exhibited a random cytoskeleton and nuclei orientation for all time points. However, when the bovine tenocytes were seeded on aligned orientated electro-spun mats, they

appeared to orientate perpendicularly to the substrate topography. The actin cytoskeleton of the cells was stained with rhodamine conjugated phalloidin; nuclei were stained with DAPI. *Arrows* indicate the orientation of the substrate topography

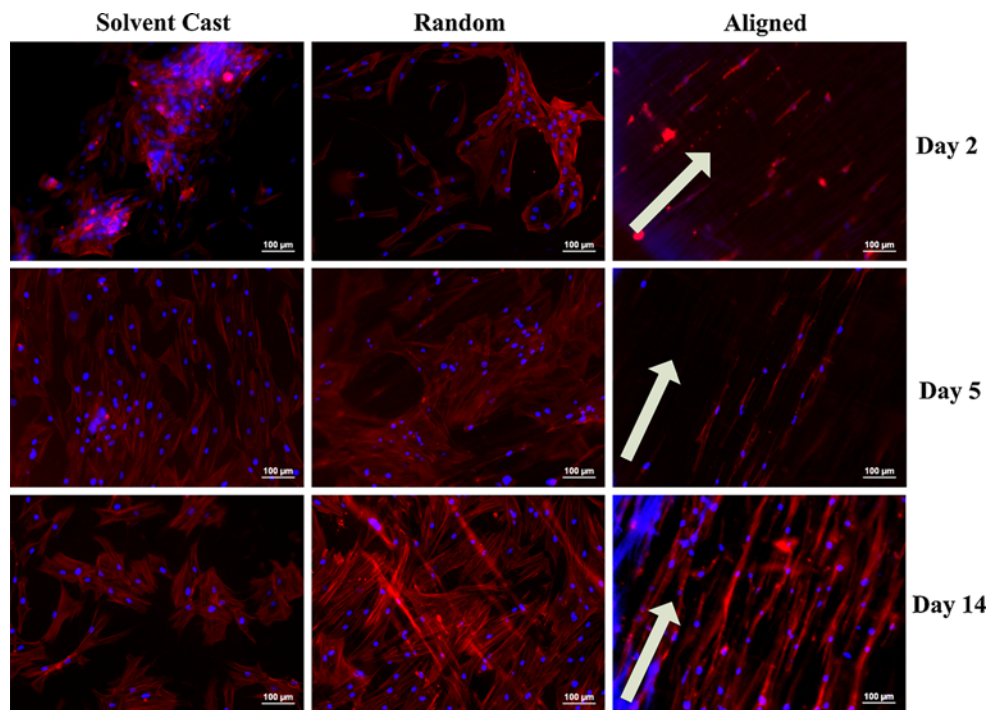


Fig. 6 Human osteoblasts were seeded on solvent casted and random orientated electro-spun mats exhibited a random cytoskeleton and nuclei orientation for all time points. However, when the human osteoblasts were seeded on aligned orientated electro-spun mats, they

appeared to orientate parallel to the substrate topography. The actin cytoskeleton of the cells was stained with rhodamine conjugated phalloidin; nuclei were stained with DAPI. *Arrows* indicate the orientation of the substrate topography

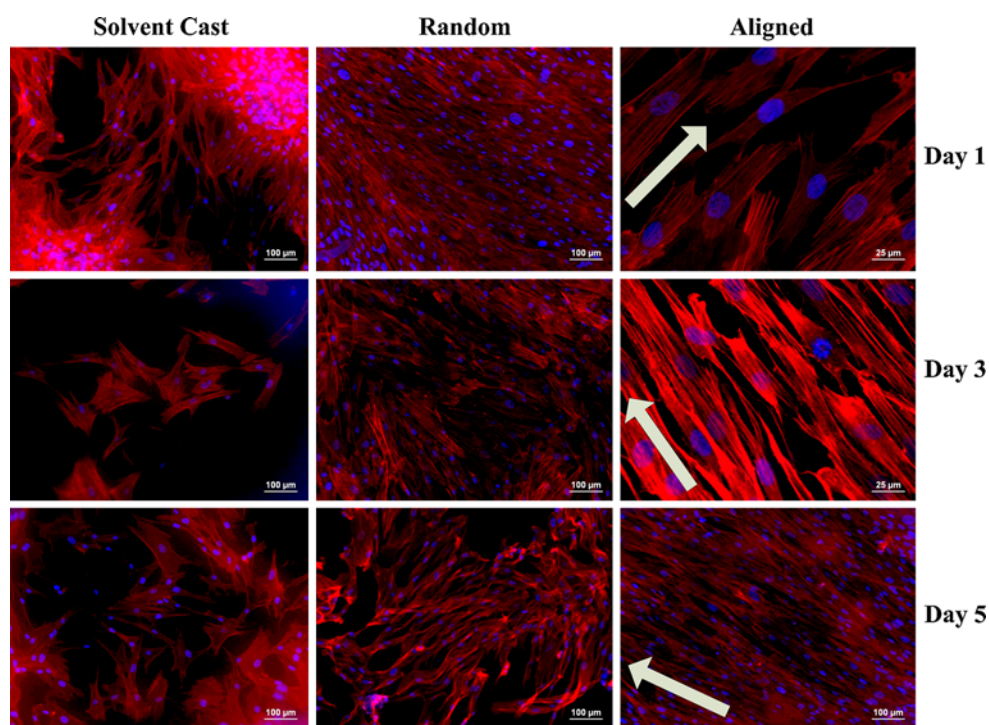


Fig. 7 Human corneal fibroblasts were seeded on solvent casted and random orientated electro-spun mats exhibited a random cytoskeleton and nuclei orientation for all time points. However, when the human corneal fibroblasts were seeded on aligned orientated electro-spun

mats, they appeared to orientate parallel to the substrate topography. The actin cytoskeleton of the cells was stained with rhodamine conjugated phalloidin; nuclei were stained with DAPI. Arrows indicate the orientation of the substrate topography

Starting with the biomechanical analysis, we found that uniaxial tensile tests of all scaffolds evaluated in this study produced stress–strain curves similar to those reported for semi-crystalline polymers that yield and undergo plastic flow [53]. Aligned and random orientated scaffolds exhibited a region of reduced stress that lasted until failure. Although it was not investigated during the current study, this yielding mechanism would imply some form of flow occurring within the fibrous structure, possibly inter-fibrillar slippage. In vivo, this mechanism is very important in the tensile deformation of connective tissues such as tendon, skin and pericardium [54–56]. Similar stress–strain curves have also been reported previously for collagen-based biomaterials [57–64] and nano-fibrous meshes [65–67]. Most important of all, the electro-spun mats produced in this study were characterised by mechanical properties that closely match those of native tissues, such as anterior cruciate ligament, Achilles tendon and skin and implantable devices [30, 62, 68–75].

Continuing with the biological analysis, we observed that the metabolic activity of human osteoblasts, corneal fibroblasts and bovine tenocytes seeded on different scaffolds increased as a function of time. Given that increasing metabolic activity is an indicator of cell proliferation, these results indicate that all scaffold conformations can support cell growth. Although no significant difference was

observed in metabolic activity of corneal fibroblasts and bovine tenocytes seeded on aligned and random orientated electro-spun mats, significant difference was observed in the metabolic activity of osteoblasts seeded on these scaffolds on day 14, indicating cell topographical preference. Fluorescent labelling of the cell cytoskeleton indicated only the aligned orientated electro-spun fibres facilitated direction cell growth of human osteoblasts and corneal fibroblasts. This finding is in agreement with previous observations for various cells and anisotropic substrates [9, 76–81]. However, of significant importance is our observation that bovine tenocytes aligned perpendicularly to the substrate topography. In previous studies, primary tenocytes had aligned parallel to the substrate topography either when grooves bigger than the cells were used or when applied load had been used along the fibre axis [82–85]. In vivo, tenocytes are elongated in shape cells arranged in a unicellular row in the space between adjacent tendon fibres [86–89], which are exposed to repeated tensile forces [90–94]. The combination of aligned collagen fibres and repeated loading may be responsible for the aligned conformation of these cells. However, when only one of these parameters is available, such as topography in the current study, we observe that the cells align perpendicularly to the underlying topography.

The emerging field of tissue engineering requires accurate delivery of bioactive and/or therapeutic molecules

to a specific location. Glycosaminoglycans and proteoglycans [95–97] or bioactive molecules such as growth factors or hormones are traditionally used to enhance biological functions of biomaterials [98–101]. However, such molecules are typically labile; the biologic half-lives of platelet-derived growth factor, basic fibroblast growth factor, and vascular endothelial growth factor are 2, 3, and 50 min, respectively, when intravenously administered [102]. As a result, the use of polymeric delivery vehicles has been advocated to encapsulate such bioactive molecules and maintain a sustained localised delivery to the target site. Current approaches to functionalise electro-spun mats are primarily based on mixing the polymer from which the scaffold is to be made with the bioactive molecule. However, this approach may affect the mechanical properties of the fibres as well as the fibre structure [23, 24]. While maintaining fibre orientation and structure we developed a co-deposition technique, whereby spinning and spraying occur simultaneously. During the deposition of electro-spun fibres, microspheres are also sprayed and trapped within the three dimensional scaffold. Microspheres are a versatile delivery vehicle used for the delivery of biomolecules. By incorporating microspheres into the network, we create an independent mechanism to tune drug delivery, while maintaining the structure of the scaffold. Drug delivery from microspheres can be easily controlled by composition and size as has been described before [103–105]. Furthermore, by using the spraying technique it is conceivable that more than one composition of microsphere may be introduced for delivery of multiple drugs. The controlled delivery of biomolecules from electro-spun/sprayed scaffolds will be the subject of future research.

5 Conclusions

Herein we ventured to investigate the influence of scaffold architecture on mechanical properties and on cell response and to develop means of sustained delivery of bioactive molecules. Our data indicate that aligned orientated fibres exhibit high stress at break values, whilst random orientated fibres exhibit high strain at break values. We identified that aligned orientated electro-spun mats facilitated parallel orientation to the underlined topography of human corneal fibroblasts and human osteoblasts. In contrast, bovine tenocytes aligned perpendicularly to the substrate topography. We speculate that the lack of mechanical loading is responsible for this; having run the experiment under tension, tenocytes would have aligned parallel to the substrate topography. We have also successfully incorporated microspheres into the three dimensional scaffold by slightly modifying the electro-spinning set-up.

Acknowledgments The authors would like to thank Mr. A. Satyam and Dr V.R. Babu for their excellent technical assistance and useful discussions. AP would like to acknowledge the Science Foundation Ireland (SFI_07/SRC/B1163) for financial support. DZ would like to acknowledge Science Foundation Ireland (SFI_09-RFP-ENM2483) and the College of Engineering for financial support. This work was also supported by Enterprise Ireland, Competence Centre for Applied Nanotechnology Project (CCIRP-2007-CCAN-0509) and by the Irish Government under the National Development Plan 2007-2013.

References

- Zeugolis DI, Chan JCY, Pandit A. Tendons: engineering of functional tissues. In: Pallua N, Suscheck CV, editors. *Tissue engineering*. Berlin: Springer; 2011. p. 537–72.
- Ionescu LC, Lee GC, Sennett BJ, Burdick JA, Mauck RL. An anisotropic nanofiber/microsphere composite with controlled release of biomolecules for fibrous tissue engineering. *Biomaterials*. 2010;31:4113–20.
- Pot SA, Liliensiek SJ, Myrna KE, Bentley E, Jester JV, Nealey PF, Murphy CJ. Nanoscale topography-induced modulation of fundamental cell behaviors of rabbit corneal keratocytes, fibroblasts, and myofibroblasts. *Investig Ophthalmol Vis Sci*. 2010; 51:1373–81.
- Hutmacher DW. Scaffold design and fabrication technologies for engineering tissues-state of the art and future perspectives. *J Biomater Sci Polym Ed*. 2001;12:107–24.
- Khademhosseini A, Langer R, Borenstein J, Vacanti JP. Microscale technologies for tissue engineering and biology. *PNAS*. 2006;103:2480–7.
- Yang L, Fitie CFC, van der Werf KO, Bennink ML, Dijkstra PJ, Feijen J. Mechanical properties of single electrospun collagen type I fibers. *Biomaterials*. 2008;29:955–62.
- Zeugolis DI, Khew ST, Yew ESY, Ekaputra AK, Tong YW, Yung L-YL, Hutmacher DW, Sheppard C, Raghunath M. Electro-spinning of pure collagen nano-fibres – Just an expensive way to make gelatin? *Biomaterials*. 2008;29:2293–305.
- Jiang X, Lim SH, Mao H-Q, Chew SY. Current applications and future perspectives of artificial nerve conduits. *Exp Neurol*. 2010;223:86–101.
- Yao L, O'Brien N, Windebank A, Pandit A. Orienting neurite growth in electrospun fibrous neural conduits. *J Biomed Mater Res B Appl Biomater*. 2009;90:483–91.
- Ladd MR, Lee SJ, Stitzel JD, Atala A, Yoo JJ. Co-electrospun dual scaffolding system with potential for muscle-tendon junction tissue engineering. *Biomaterials*. 2011;32:1549–59.
- Nerurkar NL, Sen S, Baker BM, Elliott DM, Mauck RL. Dynamic culture enhances stem cell infiltration and modulates extracellular matrix production on aligned electrospun nanofibrous scaffolds. *Acta Biomater*. 2011;7:485–91.
- Gupta D, Venugopal J, Mitra S, Giri Dev VR, Ramakrishna S. Nanostructured biocomposite substrates by electrospinning and electrospraying for the mineralization of osteoblasts. *Biomaterials*. 2009;30:2085–94.
- Li X, Xie J, Yuan X, Xia Y. Coating electrospun poly(ϵ -caprolactone) fibers with gelatin and calcium phosphate and their use as biomimetic scaffolds for bone tissue engineering. *Langmuir*. 2008;24:14145–50.
- Shields KJ, Beckman MJ, Bowlin GL, Wayne JS. Mechanical properties and cellular proliferation of electrospun collagen type II. *Tissue Eng*. 2004;10:1510–7.
- Toyokawa N, Fujioka H, Kokubu T, Nagura I, Inui A, Sakata R, Satake M, Kaneko H, Kurosaka M. Electrospun synthetic polymer scaffold for cartilage repair without cultured cells in an

- animal model. *Arthroscopy J Arthrosc Relat Surg.* 2010;26:375–83.
16. Stitzel J, Liu J, Lee SJ, Komura M, Berry J, Soker S, Lim G, Van Dyke M, Czerw R, Yoo JJ, Atala A. Controlled fabrication of a biological vascular substitute. *Biomaterials.* 2006;27:1088–94.
 17. Heydarkhan-Hagvall S, Schenke-Layland K, Dhanasopon AP, Rofail F, Smith H, Wu BM, Shemin R, Beygui RE, MacLellan WR. Three-dimensional electrospun ECM-based hybrid scaffolds for cardiovascular tissue engineering. *Biomaterials.* 2008;29:2907–14.
 18. Chai C, Leong KW. Biomaterials approach to expand and direct differentiation of stem cells. *Mol Ther.* 2007;15:467–80.
 19. Laporte LD, Shea LD. Matrices and scaffolds for DNA delivery in tissue engineering. *Adv Drug Deliv Rev.* 2007;59:292–307.
 20. Barras F, Pasche P, Bouche N, Aebischer P, Zurn A. Glial cell line-derived neurotrophic factor released by synthetic guidance channels promotes facial nerve regeneration in the rat. *J Neurosci Res.* 2002;70:746–55.
 21. Tornqvist N, Bjorklund L, Almqvist P, Wahlberg L, Stromberg I. Implantation of bioactive growth factor-secreting rods enhances fetal dopaminergic graft survival, outgrowth density, and functional recovery in a rat model of Parkinson's disease. *Exp Neurol.* 2000;164:130–8.
 22. Bensadoun J, Pereira de Almeida L, Fine E, Tseng J, Deglon N, Aebischer P. Comparative study of GDNF delivery systems for the CNS: polymer rods, encapsulated cells, and lentiviral vectors. *J Control Release.* 2003;87:107–15.
 23. Liao I, Chew S, Leong K. Aligned core-shell nanofibers delivering bioactive proteins. *Nanomedicine.* 2006;1:465–71.
 24. Huang Z-M, He C-L, Yang A, Zhang Y, Han X-J, Yin J, Wu Q. Encapsulating drugs in biodegradable ultrafine fibers through co-axial electrospinning. *J Biomed Mater Res Part A.* 2006;77A:169–79.
 25. Mundargi RC, Babu VR, Rangaswamy V, Patel P, Aminabhavi TM. Nano/micro technologies for delivering macromolecular therapeutics using poly(d, l-lactide-co-glycolide) and its derivatives. *J Control Release.* 2008;125:193–209.
 26. Meng ZX, Wang YS, Ma C, Zheng W, Li L, Zheng YF. Electrospinning of PLGA/gelatin randomly-oriented and aligned nanofibers as potential scaffold in tissue engineering. *Mater Sci Eng C.* 2010;30:1204–10.
 27. McManus MC, Boland ED, Koo HP, Barnes CP, Pawlowski KJ, Wnek GE, Simpson DG, Bowlin GL. Mechanical properties of electrospun fibrinogen structures. *Acta Biomater.* 2006;2:19–28.
 28. Wang SD, Zhang YZ, Yin GB, Wang HW, Dong ZH. Fabrication of a composite vascular scaffold using electrospinning technology. *Mater Sci Eng C.* 2010;30:670–6.
 29. Li W-J, Cooper JAJ, Mauck RL, Tuan RS. Fabrication and characterization of six electrospun poly(a-hydroxy-ester)-based fibrous scaffolds for tissue engineering applications. *Acta Biomater.* 2006;2:377–85.
 30. Kato YP, Christiansen DL, Hahn RA, Shieh S-J, Goldstein JD, Silver FH. Mechanical properties of collagen fibres: a comparison of reconstituted and rat tail tendon fibres. *Biomaterials.* 1989;10:38–42.
 31. Huang Z-M, Zhang YZ, Ramakrishna S, Lim CT. Electrospinning and mechanical characterization of gelatin nanofibers. *Polymer.* 2004;45:5361–8.
 32. Shortkroff S, Spector M. Isolation and in vitro proliferation of chondrocytes, tenocytes, and ligament cells. In: Morgan JR, Yarmush ML, editors. *Tissue engineering methods and protocols.* Totowa: Humana Press; 1999. p. 195–203.
 33. Builles N, Bechettoille N, Justin V, Ducerf A, Auxenfans C, Burillon C, Sergent M, Damour O. Development of an optimised culture medium for keratocytes in monolayer. *Biomed Mater Eng.* 2006;16:S95–104.
 34. Torbet J, Malbouyres M, Builles N, Justin V, Roulet M, Damour O, Oldberg Å, Ruggiero F, Hulmes DJS. Orthogonal scaffold of magnetically aligned collagen lamellae for corneal stroma reconstruction. *Biomaterials.* 2007;28:4268–76.
 35. Xia Y. Nanomaterials at work in biomedical research. *Nat Mater.* 2008;7:758–60.
 36. Weiss P. Experiments on cell and axon and orientation in vitro: the role of colloidal exudates in tissue organization. *J Exp Zool.* 1945;100:353–86.
 37. Rosenberg M. Cell guidance by alterations in monomolecular films. *Science.* 1963;139:411–2.
 38. Curtis A, Varde M. Control of cell behavior: topological factors. *J Natl Cancer Inst.* 1964;33:15–26.
 39. Saino E, Focarete ML, Gualandi C, Emanuele E, Cornaglia AI, Imbriani M, Visai L. Effect of electrospun fiber diameter and alignment on macrophage activation and secretion of proinflammatory cytokines and chemokines. *Biomacromolecules.* 2011;12:1900–11.
 40. Bauer AL, Jackson TL, Jiang Y. Topography of extracellular matrix mediates vascular morphogenesis and migration speeds in angiogenesis. *PLoS Comput Biol.* 2009;5:e1000445.
 41. Ridley AJ, Schwartz MA, Burridge K, Firtel RA, Ginsberg MH, Borisy G, Parsons JT, Horwitz AR. Cell migration: integrating signals from front to back. *Science.* 2003;302:1704–9.
 42. Cai K, Kong T, Wang L, Liu P, Yang W, Chen C. Regulation of endothelial cells migration on poly(d, l-lactic acid) films immobilized with collagen gradients. *Colloids Surf B Biointerfaces.* 2010;79:291–7.
 43. Xia N, Thodeti CK, Hunt TP, Xu Q, Ho M, Whitesides GM, Westervelt R, Ingber DE. Directional control of cell motility through focal adhesion positioning and spatial control of Rac activation. *FASEB J.* 2008;22:1649–59.
 44. Teixeira A, Abrams G, Bertics P, Murphy C, Nealey P. Epithelial contact guidance on well-defined micro- and nanostructured substrates. *J Cell Sci.* 2003;116:1881–92.
 45. Teixeira A, McKie G, Foley J, Bertics P, Nealey P, Murphy C. The effect of environmental factors on the response of human corneal epithelial cells to nanoscale substrate topography. *Biomaterials.* 2006;27:3945–54.
 46. Yim E, Reano R, Pang S, Yee A, Chen C, Leong K. Nanopattern-induced changes in morphology and motility of smooth muscle cells. *Biomaterials.* 2005;26:5405–13.
 47. Curtis A, Gadegaard N, Dalby M, Riehle M, Wilkinson C, Aitchison G. Cells react to nanoscale order and symmetry in their surroundings. *IEEE Trans Nanobiosci.* 2004;3:61–5.
 48. Mitragotri S, Lahann J. Physical approaches to biomaterial design. *Nat Mater.* 2009;8:15–23.
 49. Nel AE, Madler L, Velegol D, Xia T, Hoek EMV, Somasundaran P, Klaessig F, Castranova V, Thompson M. Understanding biophysicochemical interactions at the nano-bio interface. *Nat Mater.* 2009;8:543–57.
 50. Holladay C, Keeney M, Greiser U, Murphy M, O'Brien T, Pandit A. A matrix reservoir for improved control of non-viral gene delivery. *J Control Release.* 2009;136:220–5.
 51. Setton L. Reservoir drugs. Peptide-functionalized polymer nanoparticles target and bind to articular cartilage tissue, making them promising drug-delivery vehicles. *Nat Mater.* 2008;7:172–4.
 52. Kopecek J. Biomaterials and drug delivery: past, present, and future. *Mol Pharm.* 2010;7:922–5.
 53. Attenburrow GE, Bassett DC. Compliances and failure modes of oriented chain-extended polyethylene. *J Mater Sci.* 1979;14:2679–87.

54. Rigby BJ, Hirai N, Spikes JD, Eyring H. The mechanical properties of rat tail tendon. *J Gen Physiol.* 1959;43:265–83.
55. Hepworth DG, Smith JP. The mechanical properties of composites manufactured from tendon fibres and pearl glue (animal glue). *Compos Part A Appl Sci Manuf.* 2002;33:797–803.
56. Garcia Paez JM, Jorge Herrero E, Carrera Sanmartin A, Millan I, Cordon A, Martin Maestro M, Rocha A, Arenaz B, Castillo-Olivares JL. Comparison of the mechanical behaviors of biological tissues subjected to uniaxial tensile testing: pig, calf and ostrich pericardium sutured with Gore-Tex. *Biomaterials.* 2003; 24:1671–9.
57. Knight DP, Nash L, Hu XW, Haffegge J, Ho MW. In vitro formation by reverse dialysis of collagen gels containing highly oriented arrays of fibrils. *J Biomed Mater Res.* 1998;41:185–91.
58. Attenburrow GE. The rheology of leather – A review. *J Soc Leather Technol Chem.* 1993;77:107–14.
59. Wang MC, Pins GD, Silver FH. Collagen fibres with improved strength for the repair of soft tissue injuries. *Biomaterials.* 1994;15:507–12.
60. Fratzl P, Misof K, Zizak I, Rapp G, Amenitsch H, Bernstorff S. Fibrillar structure and mechanical properties of collagen. *J Struct Biol.* 1997;122:119–22.
61. Zeugolis DI, Paul GR, Attenburrow G. Cross-linking of extruded collagen fibres – a biomimetic three-dimensional scaffold for tissue engineering applications. *J Biomed Mater Res Part A.* 2009;89:895–908.
62. Pins GD, Christiansen DL, Patel R, Silver FH. Self-assembly of collagen fibers. Influence of fibrillar alignment and decorin on mechanical properties. *Biophys J.* 1997;73:2164–72.
63. Cavallaro JF, Kemp PD, Kraus KH. Collagen fabrics as biomaterials. *Biotechnol Bioeng.* 1994;43:781–91.
64. Gentleman E, Lay AN, Dickerson DA, Nauman EA, Livesay GA, Dee KC. Mechanical characterization of collagen fibers and scaffolds for tissue engineering. *Biomaterials.* 2003;24:3805–13.
65. He W, Ma Z, Yong T, Teo WE, Ramakrishna S. Fabrication of collagen-coated biodegradable polymer nanofiber mesh and its potential for endothelial cells growth. *Biomaterials.* 2005;26: 7606–15.
66. He W, Yong T, Ma ZW, Inai R, Teo WE, Ramakrishna S. Biodegradable polymer nanofiber mesh to maintain functions of endothelial cells. *Tissue Eng.* 2006;12:2457–66.
67. Kwon IK, Matsuda T. Co-electrospun nanofiber fabrics of poly(L-lactide-co-ε-caprolactone) with type I collagen or heparin. *Biomacromolecules.* 2005;6:2096–105.
68. Dunn MG, Avasarala PN, Zawadsky JP. Optimization of extruded collagen fibers for ACL reconstruction. *J Biomed Mater Res.* 1993;27:1545–52.
69. Moutos FT, Freed LE, Guilak F. A biomimetic three-dimensional woven composite scaffold for functional tissue engineering of cartilage. *Nat Mater.* 2007;6:162–7.
70. Pins G, Huang E, Christiansen D, Silver F. Effects of static axial strain on the tensile properties and failure mechanisms of self-assembled collagen fibers. *J Appl Polym Sci.* 1997;63:1429–40.
71. Pins GD, Silver FH. A self-assembled collagen scaffold suitable for use in soft and hard tissue replacement. *Mater Sci Eng C.* 1995;3:101–7.
72. Koob TJ, Hernandez DJ. Material properties of polymerized NDGA-collagen composite fibers: development of biologically based tendon constructs. *Biomaterials.* 2002;23:203–12.
73. Kato YP, Dunn MG, Zawadsky JP, Tria AJ, Silver FH. Regeneration of Achilles tendon with a collagen tendon prosthesis. results of a one-year implantation study. *J Bone Joint Surg Am Vol.* 1991;73:561–74.
74. Kato YP, Silver FH. Formation of continuous collagen fibres: evaluation of biocompatibility and mechanical properties. *Biomaterials.* 1990;11:169–75.
75. Goldstein JD, Tria AJ, Zawadsky JP, Kato KY, Christiansen D, Silver FH. Development of a reconstituted collagen tendon prosthesis. *J Bone Joint Surg.* 1989;71A:1183–91.
76. Lamers E, Frank Walboomers X, Domanski M, te Riet J, van Delft FCMJM, Luttge R, Winnubst LAJA, Gardeniers HJGE, Jansen JA. The influence of nanoscale grooved substrates on osteoblast behavior and extracellular matrix deposition. *Biomaterials.* 2010;31:3307–16.
77. Prodanov L, te Riet J, Lamers E, Domanski M, Luttge R, van Loon JJWA, Jansen JA, Walboomers XF. The interaction between nanoscale surface features and mechanical loading and its effect on osteoblast-like cells behavior. *Biomaterials.* 2010;31:7758–65.
78. Wang F, Li Z, Tamama K, Sen CK, Guan J. Fabrication and characterization of pro-survival growth factor releasing, anisotropic scaffolds for enhanced mesenchymal stem cell survival/growth and orientation. *Biomacromolecules.* 2009;10:2609–18.
79. Abu-Rub M, McMahon S, Zeugolis DI, Windebank A, Pandit A. Spinal cord injury in vitro: modelling axon growth inhibition. *Drug Discov Today.* 2010;15(11–12):436–43.
80. Schnell E, Klinkhammer K, Balzer S, Brook G, Klee D, Dalton P, Mey J. Guidance of glial cell migration and axonal growth on electrospun nanofibers of poly-[epsilon]-caprolactone and a collagen/poly-[epsilon]-caprolactone blend. *Biomaterials.* 2007; 28:3012–25.
81. Wray LS, Orwin EJ. Recreating the microenvironment of the native cornea for tissue engineering applications. *Tissue Eng Part A.* 2009;15:1463–72.
82. Chen X, Wang Z, Qin T-W, Liu C-J, Yang Z-M. Effects of micropatterned surfaces coated with type I collagen on the proliferation and morphology of tenocytes. *Appl Surf Sci.* 2008; 255:368–70.
83. Riboh J, Chong AKS, Pham H, Longaker M, Jacobs C, Chang J. Optimization of flexor tendon tissue engineering with a cyclic strain bioreactor. *J Hand Surg.* 2008;33:1388–96.
84. Wang B, Liu W, Zhang Y, Jiang Y, Zhang WJ, Zhou G, Cui L, Cao Y. Engineering of extensor tendon complex by an ex vivo approach. *Biomaterials.* 2008;29:2954–61.
85. Cao D, Liu W, Wei X, Xu F, Cui L, Cao Y. In vitro tendon engineering with avian tenocytes and polyglycolic acids: a preliminary report. *Tissue Eng.* 2006;12:1369–77.
86. Hess G, Cappiello W, Poole R, Hunter S. Prevention and treatment of overuse tendon injuries. *Sports Med.* 1989;8: 371–84.
87. Kannus P. Structure of the tendon connective tissue. *Scand J Med Sci Sports.* 2000;10:312–20.
88. Chaplin DM, Greenlee TKJ. The development of human digital tendons. *J Anat.* 1975;120:253–74.
89. Chuen FS, Chuk CY, Ping WY, Nar WW, Kim HL, Ming CK. Immunohistochemical characterization of cells in adult human patellar tendons. *J Histochem Cytochem.* 2004;52: 1151–7.
90. Boote C, Dennis S, Huang Y, Quantock AJ, Meek KM. Lamellar orientation in human cornea in relation to mechanical properties. *J Struct Biol.* 2005;149:1–6.
91. Canty EG, Kadler KE. Collagen fibril biosynthesis in tendon: a review and recent insights. *Comp Biochem Physiol A Mol Integr Physiol.* 2002;133:979–85.
92. Osborne CS, Barbenel JC, Smith D, Savakis M, Grant MH. Investigation into the tensile properties of collagen/chondroitin-6-sulphate gels: the effect of crosslinking agents and diamines. *Med Biol Eng Comput.* 1998;36:129–34.
93. Damink LHHO, Dijkstra PJ, van Luyn MJA, van Wachem PB, Nieuwenhuis P, Feijen J. Crosslinking of dermal sheep collagen using hexamethylene diisocyanate. *J Mater Sci Mater Med.* 1995;6:429–34.

94. Holmes DF, Graham HK, Kadler KE. Collagen fibrils forming in developing tendon show an early and abrupt limitation in diameter at the growing tips. *J Mol Biol.* 1998;283:1049–58.
95. Douglas T, Hempel U, Mietrach C, Viola M, Vigetti D, Heinemann S, Bierbaum S, Scharnweber D, Worch H. Influence of collagen-fibril-based coatings containing decorin and biglycan on osteoblast behavior. *J Biomed Mater Res Part A.* 2008; 84A:805–16.
96. Cao H, Xu S-Y. EDC/NHS-crosslinked type II collagen-chondroitin sulfate scaffold: characterization and in vitro evaluation. *J Mater Sci Mater Med.* 2008;19:567–75.
97. Wright KT, El Masri W, Osman A, Roberts S, Chamberlain G, Ashton BA, Johnson WEB. Bone marrow stromal cells stimulate neurite outgrowth over neural proteoglycans (CSPG), myelin associated glycoprotein and Nogo-A. *Biochem Biophys Res Commun.* 2007;354:559–66.
98. Yao C, Markowicz M, Pallua N, Magnus Noah E, Steffens G. The effect of cross-linking of collagen matrices on their angiogenic capability. *Biomaterials.* 2008;29:66–74.
99. Fontana A, Spolaore B, Mero A, Veronese FM. Site-specific modification and PEGylation of pharmaceutical proteins mediated by transglutaminase. *Adv Drug Deliv Rev.* 2008;60:13–28.
100. Shen YH, Shoichet MS, Radisic M. Vascular endothelial growth factor immobilized in collagen scaffold promotes penetration and proliferation of endothelial cells. *Acta Biomater.* 2008;4: 477–89.
101. Liman ST, Kara CO, Bir F, Yildirim B, Topcu S, Sahin B. The effects of estradiol and progesterone on the synthesis of collagen in tracheal surgery. *Int J Pediatr Otorhinolaryngol.* 2005;69: 1327–31.
102. Chen R, Mooney D. Polymeric growth factor delivery strategies for tissue engineering. *Pharm Res.* 2003;20:1103–12.
103. Chen L, Apte RN, Cohen S. Characterization of PLGA microspheres for the controlled delivery of IL-1[alpha] for tumor immunotherapy. *J Control Release.* 1997;43:261–72.
104. Mundargi RC, Srirangarajan S, Agnihotri SA, Patil SA, Ravindra S, Setty SB, Aminabhavi TM. Development and evaluation of novel biodegradable microspheres based on poly(d, l-lactide-co-glycolide) and poly([epsilon]-caprolactone) for controlled delivery of doxycycline in the treatment of human periodontal pocket: in vitro and in vivo studies. *J Control Release.* 2007; 119:59–68.
105. Chung H, Kim H, Yoon J, Park T. Heparin immobilized porous PLGA microspheres for angiogenic growth factor delivery. *Pharm Res.* 2006;23:1835–41.